Correcting Lidar Intensity Signal for Target Detection Applications

Fanar M. Abed
Marwa Mohammed Boori
Engineering College
Baghdad University\Iraq

Abstract

Laser scanning or as literary referred to as Lidar is the digital technique of obtaining information about physical objects using laser light. Airborne Lidar has shown increasing utility for feature extraction applications through enhancing the physical objects recognition process. Airborne and terrestrial Lidar provide a radiometric information alongside standard geometric information to the end user such as intensity. Intensity can be considered one of the most important parameter to identify ground features towards accurate object recognition application. This value cannot be used directly because the signal may influence by many variables during the travel between the source light (sensor) and the target. These including atmospheric, incidence angle and the target properties effects, for this reason this value should be corrected before using. This research will focus on incidence angle effect to correct Lidar intensity signal. Incidence angle is a function of the illumination direction between the sensor and the target and the point cloud orientation (normal vector). This paper, investigates the possibility of improving an approach to compute the normal vector for individual point clouds following 3D moment invariant theory. This was applied by using the commercial (OPALS), this software contain tools to compute normal vector value for individual points which were used later to compute the required incidence angle value. This leads to correct the intensity value and deliver normalized value toward improvements of automatic feature recognition applications

.

1-Introduction

1.1 Theoretical Background

Laser scanning or Lidar "light detection and ranging" is one of the new digital technology of delivering accurate 3D spatial information of the Earth's surface objects using laser light [1,16]. It is an active remote sensing system using a laser beam to scan objects and compute range between the laser unit and the ground object. There are four types of laser scanning systems (Airborne (ALS), terrestrial (TLS), mobile (MLS), and space borne (SLS)) [16]. These systems are a noncontact measurement instruments those produce a 3D digital

representation (e.g. point cloud) of the Earth surface.

All commercial laser scanning systems can provide 3D information. The 3D point clouds delivered from laser scanning systems are generated based on the integration of three individual components: a GNSS(Global Navigation Satellite System)system to provide positioning information, an INS (Inertial Navigation system) unit for altitude determination, and a laser unit to provide range (distance)information from sensor to the target [15]. Most systems are also included within build-in digital cameras to deliver imaging information. Light travelling from the laser source to the reflected target surface and back to the light detector is recorded to offers a very convenient method of evaluating distance [16]. Airborne laser scanning (ALS) is a laser scanning mounted on an airborne platform. Land cover is scanned either from a fixed wing or a helicopter airplane in order to collect all necessary information to model the topographic surface [1]. Commercial ALS systems typically operate at wavelength between 800 and 1150 nm. One advantage of ALS compared to classical photography is non-dependence on the sun as a source of light (operate day and night), and the interpretation of laser scanner data is not hampered by shadows caused by neighboring object or cloud [17]. The most Airborne and terrestrial systems provide radiometric information alongside the geometric information such as intensity for each measurement. These measurements are important for target detection applications. **Figure1** shows the dependence of intensity to recognise object.

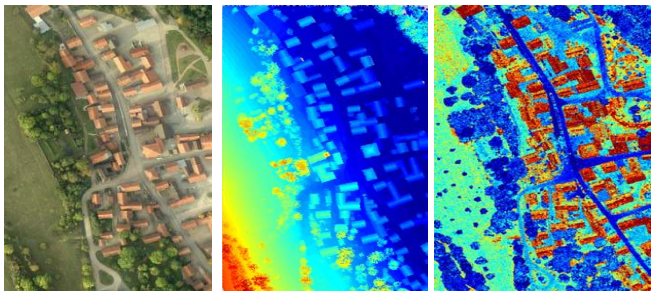

Figure 1 Dependece of intensity to recognise objects: a) RGB orthophoto; b) Image coloured by hight values; c) Image coloured by intensity values. (H. Gross, 2008).

The intensity values delivered from multiple flightlines are lake to be perfectly matched for the same ground targets due to variables affecting the laser signal when travel between the sensor and the target.

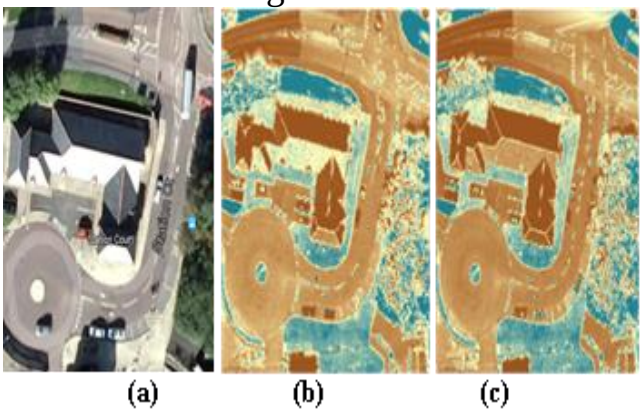

Figure (2) Dependency of the incidence angle on the intensity signals from two different flightlines: a) RGB image; b) Intensity values of flight line 1; c) Intensity values of flight line 2.

These effects are aimed to be eliminated in order to deliver accurate intensity signals to these targets. Litermature has found that incidence angle of the illumunation scatter has the major effect of mis-matching [1,2]. **Figure2** explain the difference in intensity signal delivered from two different flight lines over the same area from aerial data which used in this resarch .

In this research, the incidence angle effect was the main focus to correct intansity value and normalize it from objact orientation error.Incidence angle is a function of point cloud orientation (normal vector) and the illumination direction from the position of the sensor to the target. The 3D moment invariant theory can be used to deliver the normal vector. To apply this, an accurate normal vector routine should be used. The commercial software OPALS which stands for "Orientation and Processing of Airborne Laser Scanning data" can be used to deliver this value. The Vienna University of Technology, Department of Geodesy and Geoinformation is developing and maintaining the laser scanning (LS) software OPALS, which is a powerful tool to deliver normal vector. It is a modular program that consisting of small, well defined components referred to as "modules". Each module is accessible in three different ways: a) as command line executable from within a DOS/UNIX shell, b) as python module from within python shell, and c) as C++ code. The aim of OPALS is to provide a complete processing chain for processing airborne laser scanning data and automatic workflow for huge data volume and rapid availability of new algorithms. In OPALS, management of point cloud data is based on OPALS data manager (ODM)[11]. This software is very fast processing and flexible modules, but no graphical user interface(GUI) is provided. Therefore, an insists of a software to view the results is needed, such as GIS, QT modular, Fugro viewer etc. In this research, OPALS is utilized to deliver the normal vector values following three different algorithms towards delivering a modified lidar intensity normalization routine from incidence angle effect. Currently three different normal estimator are provided which can be mainly differentiate by their degree of robustness. simple Plane (S.P) is a standard least-squares plane adjustment offering no blunder detection (fastest method). Hence, it should be used if the normal quality is of minor concern or the focus is set on a simple roughness detection strategy. Robust Plane (R.P) detects blunders using observation weighting based on their residual. After convergence all blunder are eliminated and a final adjustment, using equally weighted observations, is performed. The robust FMCD (Fast Minimum Covariance Determinant) estimator uses an additional inverse distance weighting strategy for better approximation of the local point environment .

1.2Previos Studies of Normal Vector Computations

Incidence angle is a function of the point cloud orientation (normal vector) and the illumination direction between the sensor and the target[1]. In order to deliver the normal vector for individual points in 3D space, the environment enclosing points should be defined. Several neighborhood assumptions which deliver normal vector estimation for ALS data is available. The neighborhood of the 3D laser point is defined by the K-nearest means inside a small environment centered by the point of interest [16].There are two neighborhood environments which better define unstructured characteristic of the 3D laser points; these are the spherical and cylinder neighborhood definition [7].**Figure3** demonstrates these two environments for laser scanning point clouds. The parameter which required to define the spherical environment is the radius of the sphere. However, the cylinder environment required the radius and the height of the cylinder. The spherical based neighborhood definition is appropriate and more generic to be adopted in case of dense discrete data [2]. The majority of the existing normal vector estimation methods are based on the spherical approach [15, 5].The normal vector established by the 3D spherical volume for individual point clouds according to the Euclidian distance assumption in spherical environment following the 3D moment invariant theory which was firstly described by [7]. The definition of the 3D moment invariant was well described by [15] and later improved by [5]. The author in [13] proposed a new method to compute the normal vector based on fitting directional tangent vectors at the data point. The normal vector is derived by minimizing the variance between the associate direction tangent and the normal vector. However, [6] used the moment invariant methodology to compute the normal vector and select all the point inside a close environment and use the results to compute the incidence angle to normalize intensity value. Author [5] showed that the normal vector of the local plane of the point belonging to a segment (i.e. plane) are almost identical, therefore

several requirement for the plane fitting algorithm are introduced. This is basically to handle a high noise level and robustness at sharp surface features (i.e. plane intersection at common edges). Therefore a new method was developed which fulfills the needed requirements. This method is based on the Fast Minimum Covariance Determination (FMCD) approach described by [14]. Author [12] investigated this method to compute the normal vector in three different assumptions under the software package OPALS. Three different methods based on 3D moment invariant were investigated. In this research, it was based on commercial software (OPALS) to compute the normal vector in the 3D spherical environment .The definition of the 3D

moment invariant deliver the center of gravity and the matrix of covariance. This leads to Eigen value analysis of the individual points and compute the Eigen vector for the smallest Eigen value which represent the optimal normal vector needed.

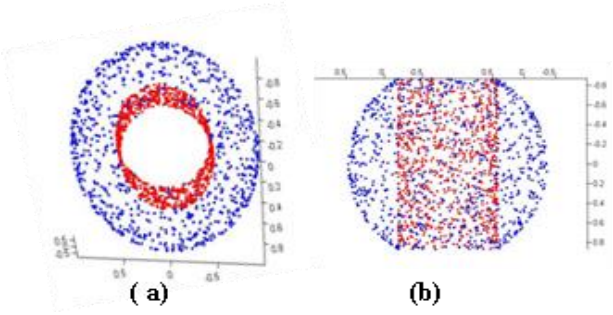

Figure (3)The two neighborhood environment definitions: a) spherical; and b) cylindrical (Wang,2013).

2- Data sets and Study sites

This research was applied on two different datasets. One of them was aerial and the second was terrestrial. The aerial dataset was from

Haltwhistle town in the north of England, U.K. The site present urban and rural areas within manmade and natural ground with a range of embankments and a variety of land cover features. It was covered by six flight lines with different overlap regions. Different targets (roof, asphalt, grass, complex roof) were selected from different flight lines to examine the applied approach. The data was captured in July 2007 from discrete pulse Optech ALTM 2050 sensor which mounted on a helicopter with high resolution of 20 points/m² and a pulse repetition rate of 50 KHz.

Figure Figure (4) The two datasets used in this research: a) Haltwistle town, UK; b) Department of Surveying Engineering, IRQ

The data set was obtained from Newcastle University for academic purposes. The terrestrial data set was captured for the department of Surveying Engineering of the University of Baghdad in Al-Jaderia district in Baghdad. The data was captured using StonexX300 laser

scanner device in April 2015. The building of the department was covered following number of steps by delivering overlap areas for calibration purposes. The device was mounted nearly (5-8)m range (this distance selected according to the designed target) from the building and use the total station and GPS to compute the coordinate of the device position. **Figure4** show both mentioned datasets.

3. Methodology

To compute the normal vector for individual points, the 3D moment invariant theory which based on the spherical environment definition was applied. The parameter which required to define the spherical environment is the radius of the sphere (radius is the distance between the first and last point in the defined spherical environment). The moment invariant theory is defined by Eq.1 [2]:

$$m_{ijk} = \int_v^n x^i y^j z^k f(x,y,z) d \qquad (1)$$

Where i, j, k ∈n, and i + j+ k are the order of the moment

n is the number of neighborhoods point

f (x,y,z) is the weighting function

v is the individual points

In this stage of the research will apply the three method over all individual points. The order of the moment was restricted to i+ j+ k<=2 following the moment definition. The center of gravity of the estimated volumetric definition can be estimated as follows:

$$\overline{x} = \frac{m_{1oo}}{m_{ooo}}, \overline{y} = \frac{m_{o1o}}{m_{ooo}}, \overline{z}\frac{m_{oo1}}{m_{ooo}} \qquad (2)$$

And the centralized moment can be computed as follow:

$$\overline{m}_{ijk} = \int_v^n (x-\overline{x})^i (y-\overline{y})^j (z-\overline{z})^k f(x,y,z) dv \qquad (3)$$

$$\overline{m}_{ijk}(x_a, y_a, z_a) = \sum_{v=1}^{v=n} (x_v-\overline{x})^i (y_v-\overline{y})^j (z_v-\overline{z})^k f(x_v, y_v, z_v) dv \qquad (4)$$

Where a is the point of interest.

The normalized moment was delivered by selecting the radius of the sphere which contain all the points

$$\widetilde{m}_{ijk} = \frac{\overline{m_{ijk}}}{R^{i+j+k} m_{ooo}} = \frac{\sum_{v=1}^{v=n}(x_v-\overline{x})^i (y_v-\overline{y})^j (z_v-\overline{z})^k f(x_v,y_v,z_v) dv}{R^{i+j+k} \sum_{v=1}^{v=n} f(x_v,y_v,z_v) dv} \qquad (5)$$

Finally symmetrical covariance matrix was computed for every centroid point as follow:

$$M = \begin{pmatrix} \widetilde{m}_{2oo} & \widetilde{m}_{11o} & \widetilde{m}_{1o1} \\ \widetilde{m}_{11o} & \widetilde{m}_{o2o} & \widetilde{m}_{o11} \\ \widetilde{m}_{1o1} & \widetilde{m}_{o11} & \widetilde{m}_{oo2} \end{pmatrix} \qquad (6)$$

Thereafter, the Eigen value was estimated for each point and the Eigen

vector for smallest Eigen value was delivered. This Eigen vector represents the optimal normal vector estimation.

The OPALS software has three different normal estimators which can be mainly differentiated by their degree of robustness. **Figure5** shows the normal vector delivered from OPALS. The first estimator was applied based on the Simple plane (SP) method which is a standard least square adjustment with no blunder detection. The second method is robust plane(RP) which detects blunders using observation weighting based on their residuals. After the elimination of all blunders, a final adjustment using equal weighted observations is utilized. The robust method is the FMCD (Fast Minimum Covariance Detection) estimator which uses an additional inverse distance weighting strategy. If the robust estimator is selected, the number of the neighbors should be increased (>10). For more details, please refer to [12]. Following that, the dot product was used to compute the incidence angle (θ) between the normal vector (N) and the elimination direction (E), and to normalized intensity value (In)following the Lambert cosine law is delivered as shown in Eq. (7).

$$In = \frac{Io}{\cos\theta} \qquad (7)$$

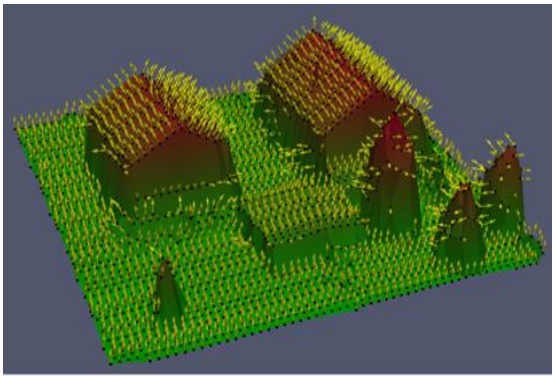

Figure (5) Normal vector estimation of buildings and vegetation visualized with Para View (OPALS, 2015)

4.Results and Discussion

In this research, to correct the intensity value from incidence angle effect, the normal vector was

computed for individual 3D points following three different methods. Ten points have been utilized as neighbors applied on specific selected targets from both datasets.

Manmade and natural features were

selected in aerial dataset from overlap areas between two adjacent flight lines (asphalt road, house roof, complex roof, terrain, etc.).

Figure6 shows the normal vector results delivered from the mentioned three methods of complex surface from house roof targets from aerial dataset.

Using the trajectory information, illumination direction can be computed by estimating the vector from the sensor to the target. This leads to estimate the incidence angle value for individual point clouds following vector dot product in 3D space. To

correct the intensity value, the Lambert cosine law was applied to compute the normalized intensity for each point in both flight lines.

Figure7 shows an interest area colored based on intensity value from two flight lines, difference map was computed from the original and the normalized intensity signal in the mentioned three methods. The difference map is the difference of intensity value from multiples flight lines, however, the maps colored based on intensity value for individual interest areas in the overlap region delivered from all flight lines and subtracting these map from each other. To approve the output results, statistical analysis was adopted for all the selected targets and the interest areas in order to deliver an accurate value of the match between the signals from overlapping flight lines as compared with the original signals. This can deliver an indication about the elimination in the discrepancies between overlapping flight lines after intensity correction following three different methods. Two -sample T-test is used to compare intensity values delivered from three normalization methods before and after correction. The 2-sample T-test was designed to compare means of two samples after checking the variance analysis based on F-test or levene's test following P-value analysis [12]. If the P-value greater than 0.05 this mean the two data sets have equal variances thus they are both similar and the statistical hypothesis can be accepted. Following difference map analysis, the comparison was based on comparing between P-values delivered after normalization with those delivered from the original signals to find the progress percentage .

If the difference was too small referred by P-values, T-values can be adopted for analysis instead such as the case in some targets selected in this research. Please refer to [12]for further details about P and T values. Table 1 and Table 2 show the P&T values results delivered from T-test analysis to each selected target in both aerial and terrestrial data sets respectively. The results from statistical analyses show that the difference map have delivered lower discrepancies and thus better match between flight lines after correction when using FMCD algorithm to compute the normal vector in a comparison with both the simple surface (S. P.) and R.P methods over truly planar surfaces. However, when the surface was complex, the results show that the S.P and R.P method scan deliver better results than FMCD algorithms. The results from the S.P and R.P methods were nearly identical over all selected targets. Figure (8) shows samples of the selected targets in this research.

It can be noticed from Table 1 and 2 that the T-value decreases after correction from all methods comparing with the original difference in intensity value. This means that the difference in intensity from two flight line was

minimized after correcting the intensity signals from incidence angle effect.

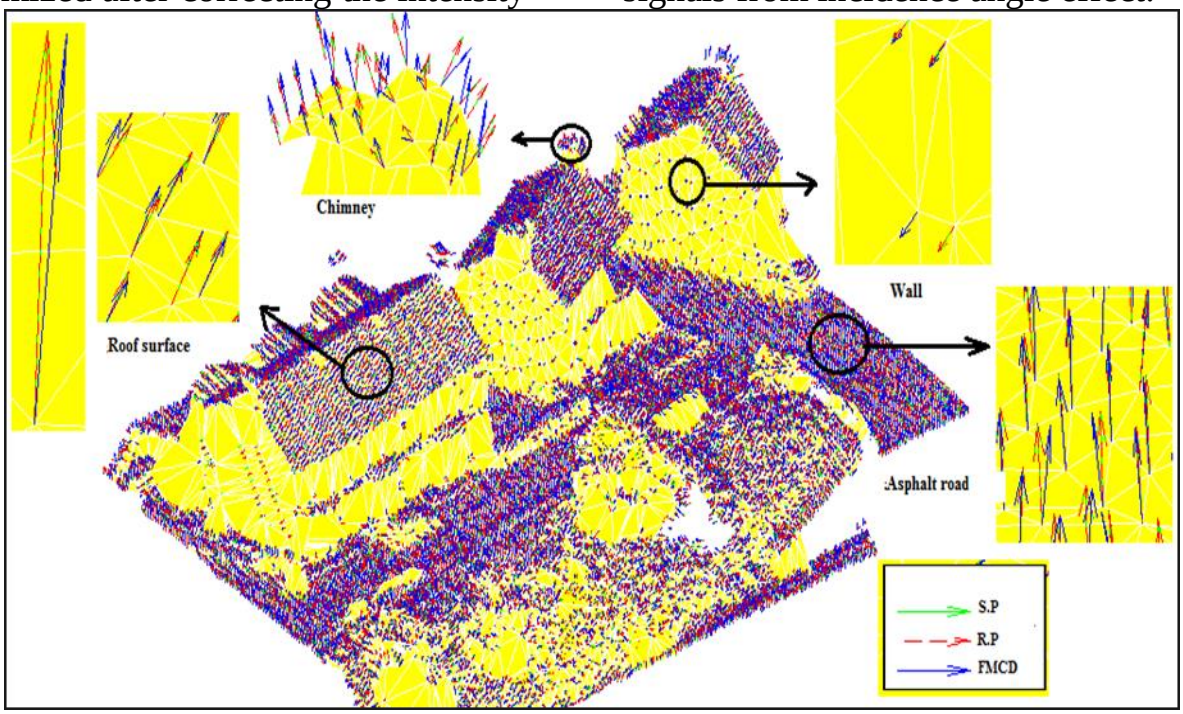

Figure (6) Normal vector results of the normal vector delivered from three methods. Where green normal vector is refering to S.P, red normal vector is referring to R.P, and blue normal vector is referring to FMCD.

Table (1) Shows the results delivered from statistical analysis following 2-sample T-test of aerial dataset (Haltwhistle town).

Target	No. of Points		Original		Simple plane method		Robust plane method		FMCD method	
	Flightline1	Flightline2	P- value	T-value	P- value	T-value	P-value	T-value	P-value	T-value
Roof house1	250	821	0	-10.80	0	-4.22	0	-4.22	0	-1.76
Roof house2	563	1165	0	-10.87	0	-6.64	0	-6.64	0	0.043
Complex roof1	1647	3354	0	-20.17	0	-13.29	0	-13.29	0	-15.18
Complex roof2	1432	3443	0	-22.60	0.106	1.62	0.106	1.62	0	-5.68
Asphalt road1	1071	2729	0	-21.79	0	-19	0	-19	0	-23.55
Asphalt road2	1442	3501	0	-15.67	0.344	0.95	0.344	0.95	0	-7.20
Terrain slop1	582	1049	0	-55.35	0	-30.87	0	-30.87	0	-21.48
Terrain slop2	1084	2537	0	-70.57	0	-7.19	0	-7.19	0.474	-0.72

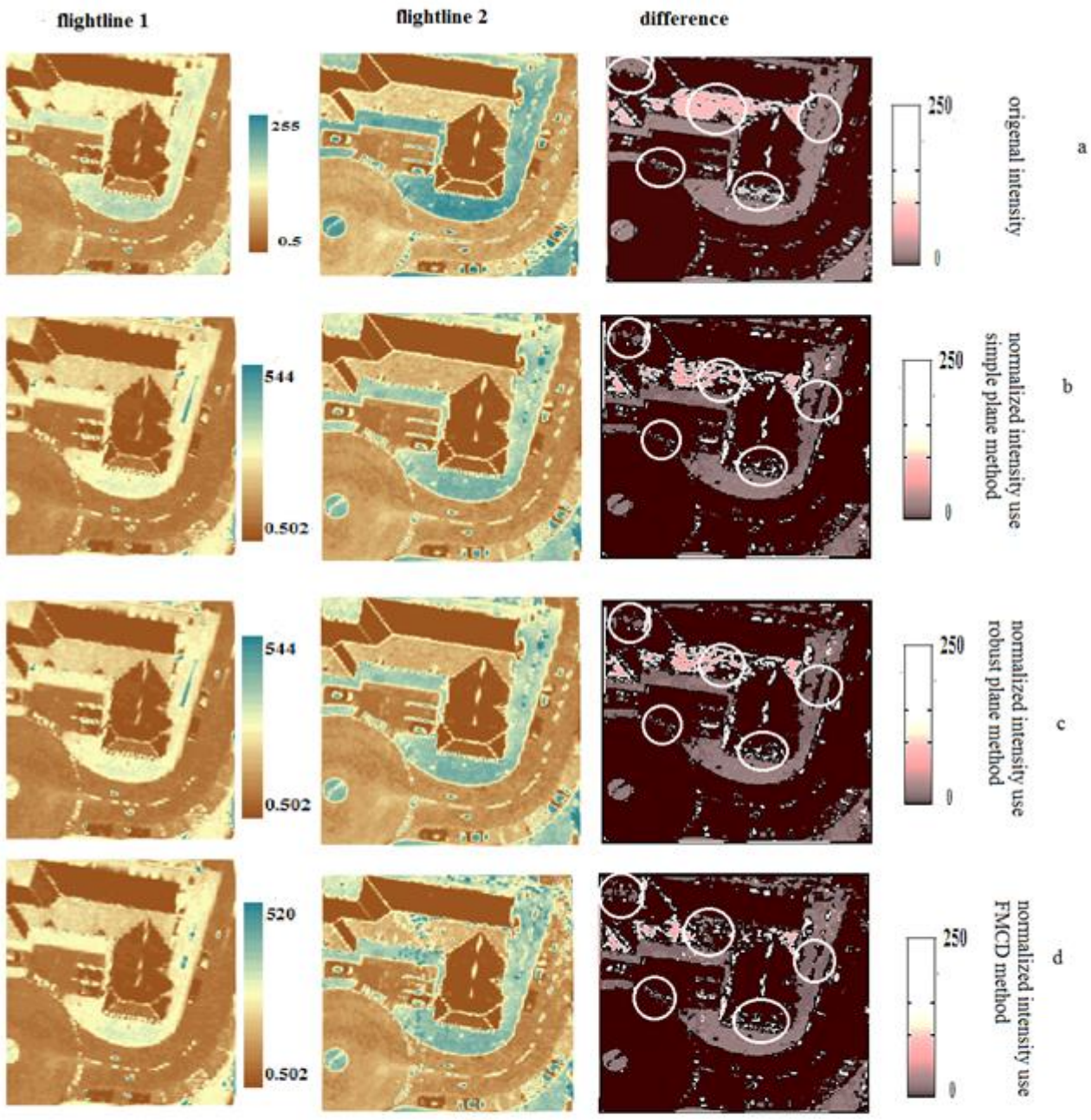

Figure (7) The selected interest area from aerial dataset colored by intensity value: a) Origenal intensity from two flight lines and their difference map; b) Normalized intensity from two flight lines and their difference map using S.P method; c) Normalized intensity from two flight lines and their difference map using R.P method; d) Normalized intensity from two flight lines and their difference map using FMCD method.

Table (2) Show the statistical analysis results of terrestrial data set (Surveying Engineering Department).

Target	No. of Points		Original			Simple plane method			Robust plane method			FMCD method		
			Flight line	P-value	T-value	Flight line	P- value	T-value	Flight line	P-value	T-value	Flight line	P-value	T-value
Grass	strip1	177063	1&2	0	-577.15	1&2	0.6	0.48	1&2	0.6	0.48	1&2	0.144	-1.46
	Strip2	14463	1&3	0	-279.19	1&3	0.363	0.91	1&3	0.363	0.91	1&3	0.128	1.52
	Strip3	3847	2&3	0	-14.28	2&3	0	9.11	2&3	0	9.11	2&3	0	5.23
ComplexWall	Strip1	25651	1&2	0	-34.45	1&2	0.001	-3.40	1&2	0.001	-3.40	1&2	0	-4.68
	Strip2	19663	1&3	0	-27.84	1&3	0.004	-2.90	1&3	0.004	-2.90	1&3	0	-6.55
Plate	Strip1	405738	1&2	0	53.78	1&2	0.002	3.13	1&2	0.002	3.13	1&2	0.268	-1.11
	Strip2	122617	1&3	0	91.96	1&3	0	23.23	1&3	0	23.23	1&3	0	14.71
	Strip3	64286	2&3	0	37.05	2&3	0	7.47	2&3	0	7.47	2&3	0.150	1.44
Plate /boy	Strip1	43523	1&2	0	20.85	1&2	0	4.12	1&2	0	4.12	1&2	0.097	-1.66
	Strip2	15046	1&3	0	44.01	1&3	0	8.61	1&3	0	8.61	1&3	0	8.38
	Strip3	8143	2&3	0	19.95	2&3	0	11.44	2&3	0	11.44	2&3	0.436..	0.78
Column	Strip1	19050	1&2	0	14.85	1&2	0	8.14	1&2	0	8.14	1&2	0	10.79
	Strip2	9924	1&3	0	18.20	1&3	0	9.53	1&3	0	9.53	1&3	0	12.35
	Strip3	----	2&3	------	------	2&3	------	------	2&3	------	------	2&3	-----	-----
Balcony	Strip1	33220	1&2	0	-16.52	1&2	0.276	1.09	1&2	0.276	1.09	1&2	0.096	1.67
	Strip2	10607	1&3	0	-15.60	1&3	0.001	3.42	1&3	0.001	3.42	1&3	0.184	1.33
	Strip3	6285	2&3	0	-5.95	2&3	0.128	1.52	2&3	0.128	1.52	2&3	0.938	-0.08
Balcony/window	Strip1	2285	1&2	0	12.14	1&2	0.45	-0.74	1&2	0.45	-0.74	1&2	0.917	-0.10
	Strip2	3274	1&3	0	28.78	1&3	0.83	0.21	1&3	0.83	0.21	1&3	0.091	1.69
	Strip3	4167	2&3	0	19.50	2&3	0.293	1.05	2&3	0.293	1.05	2&3	0.298	1.04

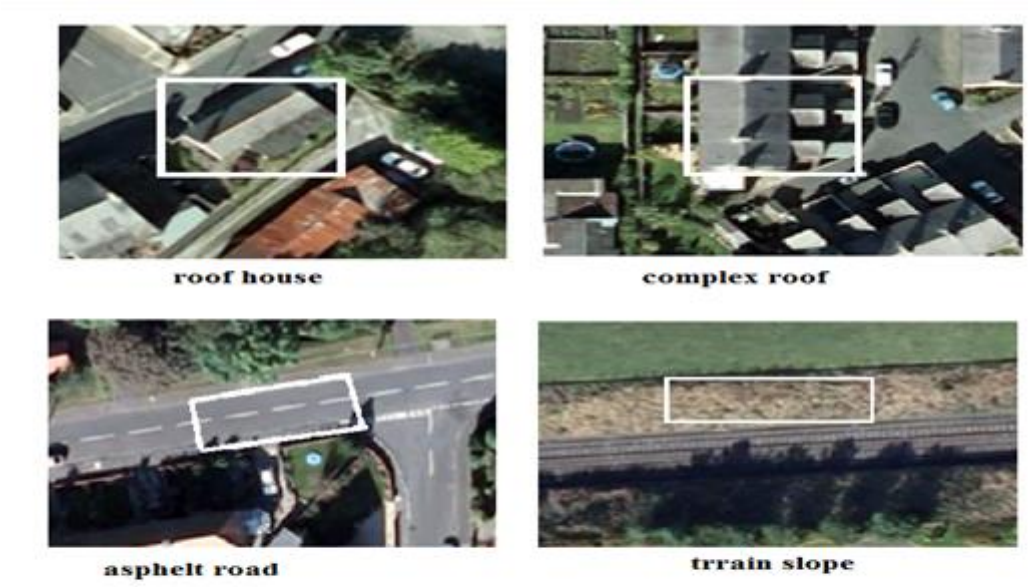

Figure (8) Sample RGB orthophotos of the selected targets.

5. Conclusions.

In this paper, two different lidar platforms, correcting lidar intensity signals from incidence angle effect based on three different algorithms for normal vector computations were introduced and demonstrated. Following three different normal vector computation methods, it was found that the S.P and R.P methods can deliver nearly the same results over different targets with various properties. However, the FMCD method delivers the best results over all simple planar surfaces. When the plane is complex both S.P and R.P method scan deliver better results and some exceptions have notices which might happened due to noise effects. After applying the Lambert cosine law to reduce the incidence angle effect towards lidar intensity correction, discrepancies between signals from flight lines have decreased successfully. Better match between overlapping flight lines was delivered after intensity correction process. This was demonstrated and validated following visual and statistical analysis. This can be clearly seen for all selected targets from Table 1 and Table 2 of both datasets. Further, the visual improvements through difference map analysis can be seen in Figure (7) over the selected interest area from the aerial dataset. This is

clearly visualized in the regions highlighted with the white circles with the difference delivered between the original and the corrected signals from the three applied methods. Following these achievements, an improved intensity correction method will be introduced in future work and compare with the presented results towards more generic and accurate lidar intensity signals methodologies for target detection and object recognition applications.

6- Acknowledgements

We would like to a acknowledge Vienna University of Technology, department of Geodesy and Geoinformation in Austria for providing the OPALS commercial software, and also for their help and guidance through the processing stages. The authors would also like to thank Newcastle University (UK) for providing Haltwhistle dataset.

7- References

1- Abed, F. M., Mills, J. P. and Miller, P. E. (2011), 'Calibration of full-waveform ALS data based on robust incidence angle estimation', International Archives of Photogrammetry, Remote Sensing and Spatial Information Sciences, 38 (5/W12), 6 p.

2- Abed, F. M., Mills, J. P. and Miller, P. E., 2014. “Calibrated Full-Waveform Airborne Laser Scanning for 3D Object Segmentation”, Remote Sensing Journal, (6), 4109-4132pp.

3- Coren, F. and Sterzai, P. (2006), " Radiometric correction in laser scanning", International journal of remote sensing, 27(15), pp.3097-3104.

4- Dorninger, P. and Nothegger, C., 2007. 3D Segmentation of Unstructured Point Clouds for Building Modeling. In: IAPRS XXXVI Part 3/W49A, pp. 191-196.

5- Gross, H. and Thoennessen, v. (2006), "Extraction of lines from laser point clouds", International Archives of photogrammetry, remote sensing and spatial information sciences, 36(3) pp. 86-91.

6- Gross, H. Julzi; B. and Thoennessen U.(2008), "Intensity normalization by incidence angle and range of full-waveform lidar data", International Archives of photogrammetry, remote sensing and spatial information sciences, 37(B4), pp.405-411.

7- Hu, M.-K. (1962) , ‘Visual pattern recognition by moment invariants', IRE Transactions

on Information Theory, 8 (2), pp. 179-187.

8- Jin Wang , 2013 " Block-to-Point Fine Registration in Terrestrial Laser Scanning" Geodätisches Institut , Leibniz Universität Hannover, D-30167 Hannover, Germany ,pp .6921-6937

9- Lee, I. and Schenk, T. (2001), '3D perceptual organization of laser altimetry data', International Archives of Photogrammetry, Remote Sensing and Spatial Information Sciences, 34 (3/W4), pp. 57-65.

10- Maas, H.-G. and Vosselman, G. (1999), 'Two algorithms for extraction building models from raw laser altimetry data', ISPRS Journal of Photogrammetry and Remote Sensing, 54 (2-3), pp. 153-163.

11- Mandlburger, G., Otepka, J., Karel, W., Wagner, W. and Pfeifer, N. (2009), 'Orientation and processing of airborne laser scanning data (OPALS) - concept and first results of a comprehensive ALS software', International Archives of Photogrammetry, Remote Sensing and Spatial Information Sciences, 38 (3/W8), pp. 55-60.

12- Montgomery, D. C. (2005), Design and analysis of experiments. Chichester, UK: Willy-BlackWell.

13- Ou Yang, D. and Feng , H.-Y. (2005), 'On the normal vector estimation for point cloud data from smooth surfaces', Computer-Aided Design, 37 (10), pp. 1071-1079.

14- Rousseuw, P. J., van Driessen, K., 1999. A fast algorithm for the minimum covariance determinant estimator. Technimetrics, pp. 212-223.

15- Shan, J. and Toth, C. K. (2009), Topographic laser ranging and scanning - principles and processing. FL, USA: Taylor & Francis.

16- Vosselman, G. and Maas, H.-G. (2010), Airborne and terrestrial laser scanning. Scotland, UK: Whittles Publishing.

17- Wagner, W. (2005), 'Physical principles of airborne laser scanning' .Institute of Photogrammetry and Remote Sensing, Vienna University of Technology, 40 p.

تصحيح شدة الطاقة الليزرية في تطبيقات اكتشاف الاهداف

فنار منصور عبد
مدرس
مروة محمد بوري
قسم هندسة المساحة
كلية الهندسة – جامعة بغداد /العراق

الخلاصة

المسح الليزري هوتقنية رقمية حديثة تمكننا من الحصول على معلومات دقيقة عن الاجسام الارضية باستخدام ضوء الليزر. يعتبر نظام المسح الليزري الجوي واحد من اكثرالانظمة استخداما في عمليات تمييز العوارض. ان المسح الليزري الجوي يزود المستخدم بمعلومات فيزيائية اضافية اضافة الى المعلومات الهندسية ومن هذه المعلومات هي شدة الطاقة الليزرية المرتدة من الاجسام. هناك عدة دراسات اثبتت اهمية هذه المعلومات الاضافية في امكانية تمييز الاهداف لكن الاستخدام المباشر لهذه القيمة لا ينصح به وذلك لان الليزر يتعرض لعدة عوامل تؤثر على شدته اثناء رحلته من المتحسس الى الاهداف. هذه العوامل تشمل تأثير الغلاف الجوي وطبيعة الاهداف وزاوية السقوط وغيرها لذلك ينبغي تصحيح هذه القيمة من تأثير تلك العوامل قبل استخدامها في عمليات هندسية دقيقة هذا البحث يهدف الى دراسة تأثير زاوية السقوط على هذه القيمة و تصحيحها. زاوية السقوط هي الزاوية المحصورة بين المتجه العمودي لكل نقطة وبين المتجه الذي يربط المتحسس بالهدف. يتضمن هذا البحث تحسين الطرق المألوفة في حساب المتجه العمودي لكل نقطة بتطبيق نظرية (D moment invariant3) والمستخدمة في البرنامج التجاري (OPALS) في أحدى موديلاته والذي تم الحصول عليه من جامعة فيينا في النمسا. بعد الحصول على قيمة المتجه العمودي تم حساب زاوية السقوط وتصحيح شدة الطاقة الليزرية باستخدام قانون لامبرت لنتمكن من تحسين تمييز العوارض أوتوماتيكيا.